CORROSION BEHAVIOR OF AUSTENITIC AND FERRITIC STEELS IN SUPERCRITICAL WATER

XIN LUO*, RUI TANG, CHONGSHENG LONG, ZHI MIAO, QIAN PENG and CONG LI[2]
National Key Laboratory for Nuclear Fuel and Materials, Nuclear Power Institute of China,
P.O. Box 436, Chengdu, Sichuan, PR China 610041
[2]China Nuclear Power Technology Research Institute
1788 Xi Huan Road, Suzhou, PR China 215004
*Corresponding author. E-mail : xin8285@163.com

Received June 15, 2007
Accepted for Publication November 15, 2007

The general corrosion behavior of austenitic and ferritic steels (316L, 304, N controlled 304L, and 410) in supercritical water is investigated in this paper. After exposure to deaerated supercritical water at 480 ºC/25 MPa for up to 500 h, the four steels studied were characterized using gravimetry, scanning electron microscopy/energy dispersive X-ray spectroscopy (SEM/EDS), X-ray photoelectron spectroscopy (XPS), and X-ray diffraction (XRD). The results show that the 316L steel with a higher Cr and Ni content has the best corrosion-resistance performance among the steels tested. In addition to the oxide layer mixed with Fe_3O_4 and $(Fe,Cr)_3O_4$ that formed on all the samples, a Fe_3O_4 loose outer layer was observed on the 410 steel. The corrosion mechanism of stainless steels in supercritical water is discussed based on the above results.

KEYWORDS : Stainless Steel, Supercritical Water, Corrosion, Oxide Layer

1. INTRODUCTION

The supercritical water reactor (SCWR) is one of the six reactor concepts that have been selected for future Generation IV nuclear reactor systems [1]. Operating above the thermodynamic critical point of water (374 ºC, 22.1 MPa), the SCWR is a promising advanced nuclear system due to its high thermal efficiency (approximately 44~45%) and considerable plant simplification [2,3]. Since the supercritical water coolant has both liquid-like and gas-like characteristics and a higher temperature than the water coolant of conventional light water reactors (LWRs), corrosion of the structural materials commonly used in LWRs and fossil power plants under SCWR conditions has been identified as a critical problem [4,5].

Owing to the good corrosion resistance and low cost, austenitic and ferritic stainless steels, which are widely used as structural materials in conventional nuclear reactors [6], have been considered as promising candidate materials for SCWR [7]. However, the existing data on the corrosion of stainless steels in a pure supercritical water environment corresponding to SCWR conditions is sparse; therefore, further investigation is necessary [8]. Recently, most of the studies by Allen *et al*. [9-11] have focused on the corrosion behavior of 9-12% Cr F/M steels, such as T91, HT9, and HCM12A, exposed to supercritical water at 500 ºC/25 MPa with different oxygen contents. It was found that the oxide layers consisted primarily of a Fe_3O_4 outer layer and an inner oxide layer with a $(Fe,Cr)_3O_4$ spinel structure.

Of the major constituent elements of stainless steels, Cr can promote the formation of a protective surface oxide and Ni can enhance the stability of the protective oxide [12]. 304 steel is commonly used in the manufacture of larger reactor vessel internals in pressurized water reactor environments [13]. In order to eliminate the harmful effect of carbon on its corrosion resistance, N controlled 304L was developed with a low carbon content and a controlled nitrogen content in a solution annealed condition [14]. To compare the corrosion resistance of stainless steels with different compositions and to understand the effects of alloy elements on corrosion in SCWRs, the general corrosion behavior of the austenitic steels 316L, 304, N controlled 304L, and the ferritic steel 410 in SCW at 480 ºC under a pressure of 25 MPa for up to 500 h are studied in this paper.

2. EXPERIMENTAL

Three types of cold rolled austenitic steels (316L, 304,

N controlled 304L) and one ferritic steel (410) were used in this study. The chemical compositions of the steels are listed in Table 1. Figure 1 shows the microstructure of the N controlled 304L steel. The geometry of the test samples was 40 mm ×20 mm with a thickness of 2 mm. The samples were first polished with SiC abrasive papers (grit no. 800) and then cleaned ultrasonically using acetone.

The deaerated supercritical water exposure experiments were performed in a supercritical autoclave at conditions of 480 ºC and 25 MPa for 50, 120, 220, 350, and 500h. After removing the oxide film using the alkaline permanganate-ammonium citrate (APAC) method, the corrosion behavior of the steels was evaluated in terms of weight loss. The oxide morphology and thickness were characterized using a SEM. The oxide structure was analyzed using EDS, XPS, and XRD techniques.

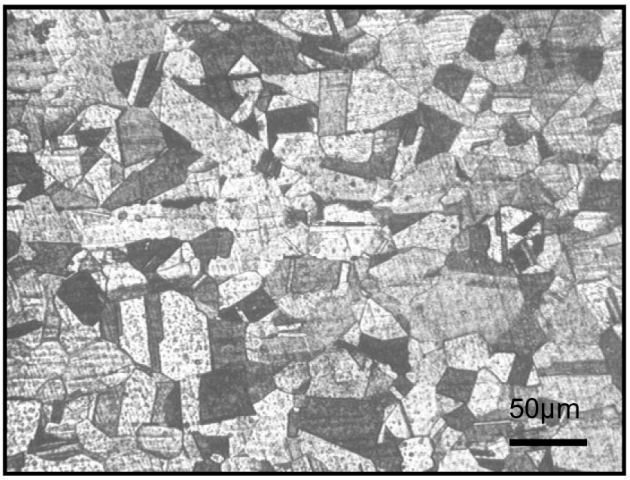

Fig. 1. The Microstructure of N Controlled 304L Steel

3. RESULTS AND DISCUSSION

3.1 Oxide Morphology

The surface morphology of the oxide layer formed on the steel samples exposed to 480 ºC supercritical water (SCW) is shown in Fig. 2. It can be seen on the surface of 316L and 410 that the granular oxide dispersed and grew as the exposure time increased. The oxide on 316L did not grow uniformly, and its particle size was smaller than that of the 410 steel. A porous oxide layer composed of large polyhedral grains was generated on the surface of the 410 steel and reveals the reason of the greater weight loss where oxygen can be diffused into the samples easily through the porous layer. The low magnification image (Fig. 3) of 410 shows that the distribution of this larger granular oxide is not uniform, which may be a result of the oxide spallation.

Figure 4 shows the cross-sectional morphology of the oxide layer. Although the extensive oxide spallation results in unreliable measurements of the oxide scale thickness using the SEM images, it can be observed that the oxide layers of 304 and N controlled 304L are much thinner than those of 316L and 410. However, it cannot be confirmed that the steel with a thinner oxide layer has a better corrosion resistance due to the extensive oxide spallation; the N controlled 304L sample may experience a quicker oxide spallation rate than the other samples.

3.2 Corrosion-resistance Performance

Due to the oxide spallation, the corrosion resistance was analyzed by weight loss. Figure 5 shows the weight loss of the four steel samples after the treatment to remove oxide film after the exposure to SCW at separate time intervals. It can be seen that the austenitic steels have a better corrosion resistance than the ferritic steel. Among the austenitic steels, 316L showed the best corrosion resistance, and the general corrosion rate was 0.0061 $mm \cdot a^{-1}$. This indicates that Cr and Ni are the key elements to increase the corrosion resistance, and Mo is also

Table 1. Chemical Composition of Steel Specimens Used in this Study

Specimens	Composition											
	C	Si	Mn	P	S	Cr	Ni	Mo	N	Cu	B	Co
316L	0.025	0.29	1.41	0.017	0.015	17.22	14.14	2.25	-	-	-	-
304	0.06	0.48	1.45	0.024	0.005	18.25	8.16	-	-	-	-	-
N controlled 304L	0.018	0.58	1.21	0.018	0.007	19.40	9.35	-	0.089	0.062	≤0.0015	0.028
410	0.12	0.50	0.63	0.023	0.002	11.85	-	-	-	-	-	-

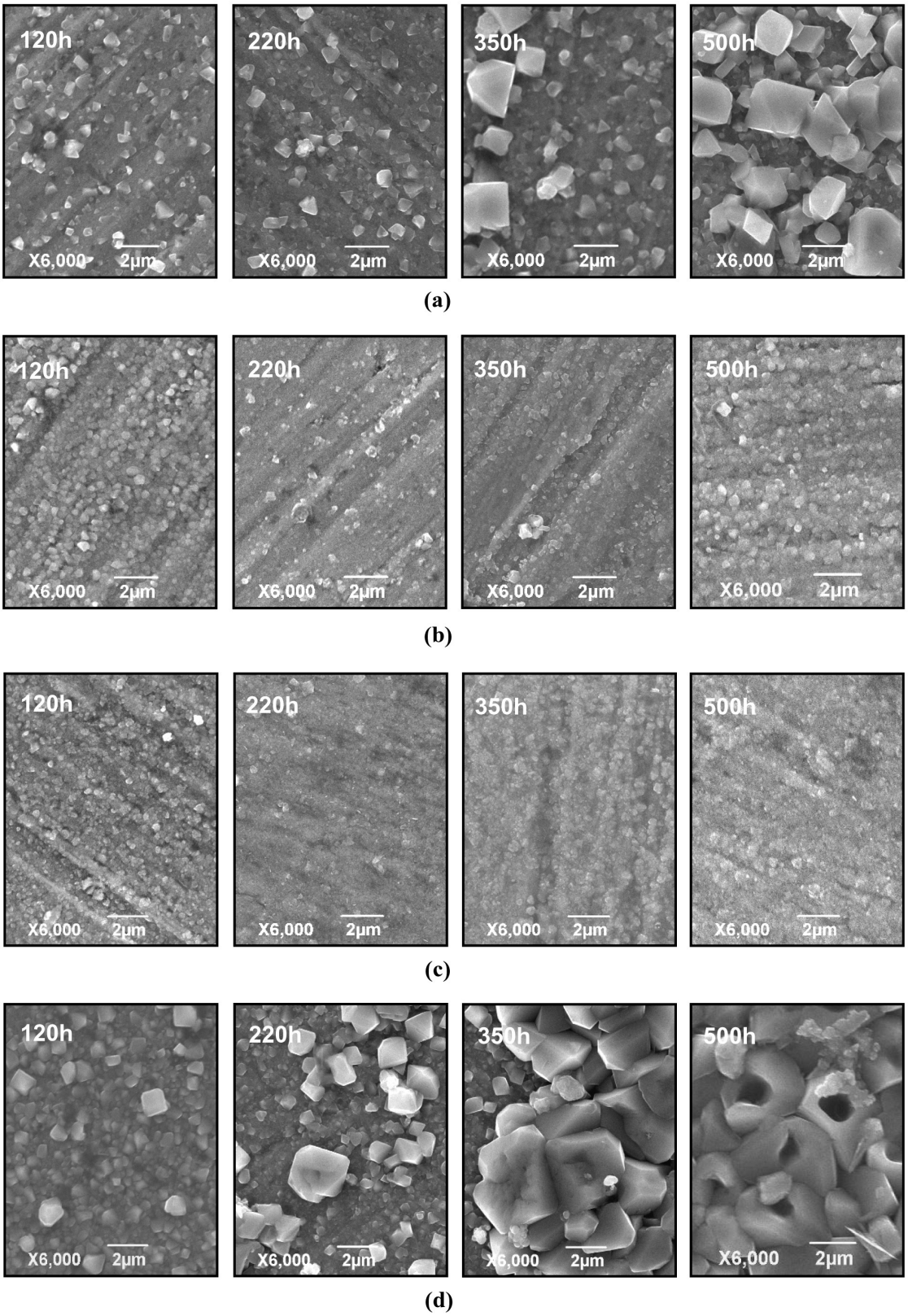

Fig. 2. SEM Images of the Surface Morphologies of the Oxide Layer on Stainless Steels Exposed to SCW at 480 ºC /25 MPa: (a) 316L, (b) 304, (c) N Controlled 304L, and (d) 410

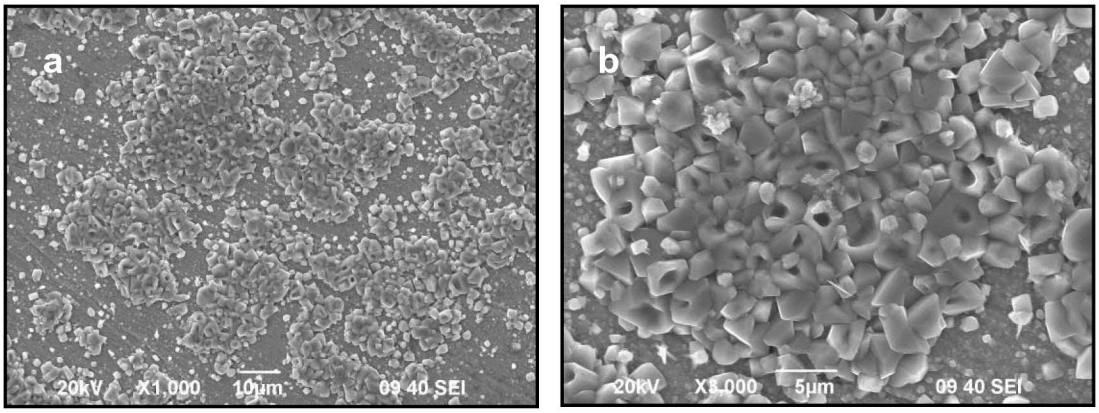

Fig. 3. SEM Images of the Surface Morphology of the 410 Samples Tested for 500 h at Low Magnifications: (a) 1000 × and (b) 3000 ×

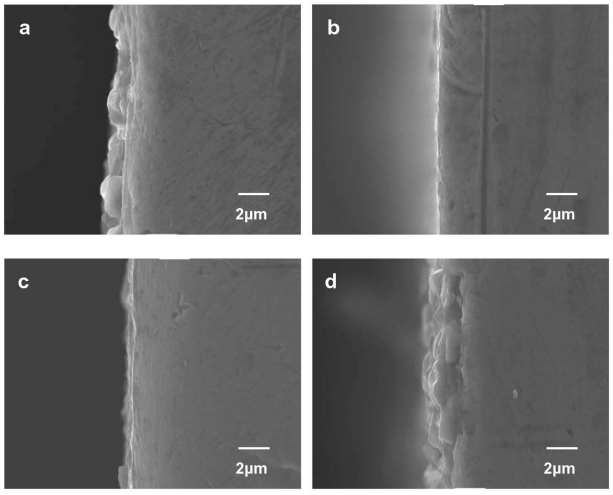

Fig. 4. Cross-Section of Oxide Layers Formed on the Stainless Steels Samples Tested Over 500 h: (a) 316L, (b) 304, (c) N Controlled 304L, and (d) 410

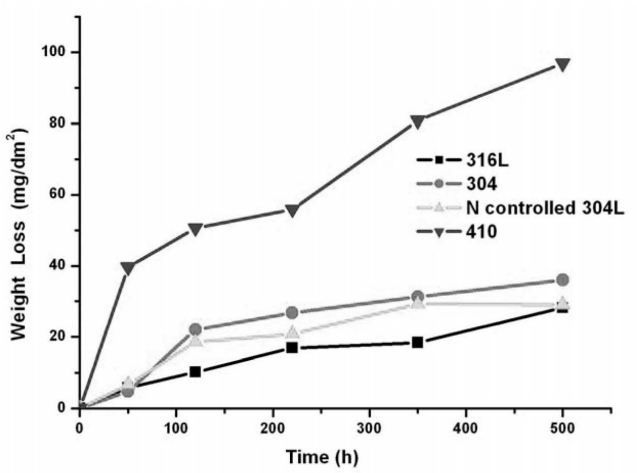

Fig. 5. Weight Loss Data as a Function of the Exposure Time for the Samples Exposed to SCW at 480 ºC/25 MPa After Dissolution of the Oxide Layer Using a Permanganate Solution

effective in improving corrosion resistance. N controlled 304L has a lower corrosion rate than 304, which may be attributed to its higher Cr content and the cooperation of trace elements such as N and Cu. Furthermore, the oxide spallation of 304 and N controlled 304L steel appears to be due to the lower Ni content.

3.3 Oxide Structure

Using the EDS line-scan technique, the composition profiles across the thickness of the oxide layers are shown in Fig. 6. The major element concentrations (O, Fe, Ni, and Cr) display similar distributions in the oxide scale of the 304 and N controlled 304L samples, and the surface oxide appeared to be a single layer, as shown in Figs. 6(b) and 6(c). The oxide layer of 316L also appears to be a single layer, in which Fe, Cr, and Ni have similar distributions, excepting higher oxygen concentrations. As shown in Fig. 6(d) and the EDS results (Fig. 7), the oxide layer of the 410 steel appears to be composed of two layers: an Fe-rich outer oxide layer and a Cr-rich inner oxide layer.

Figure 8 shows the Fe 2p, O 1s spectra of the surface film of the four samples. The peak of the Fe 2p core level spectrum at 710.7 and 724.2 corresponds to the iron in

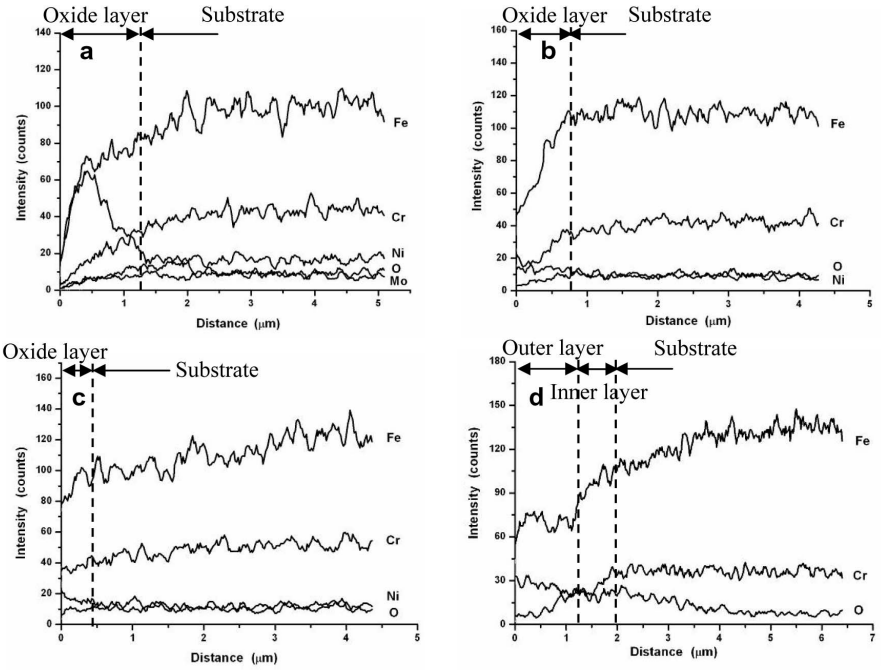

Fig. 6. EDS Line-Scan Profiles Over a Cross-Section of Stainless Steels Samples Tested After 500 h: (a) 316L, (b) 304, (c) N Controlled 304L, and (d) 410

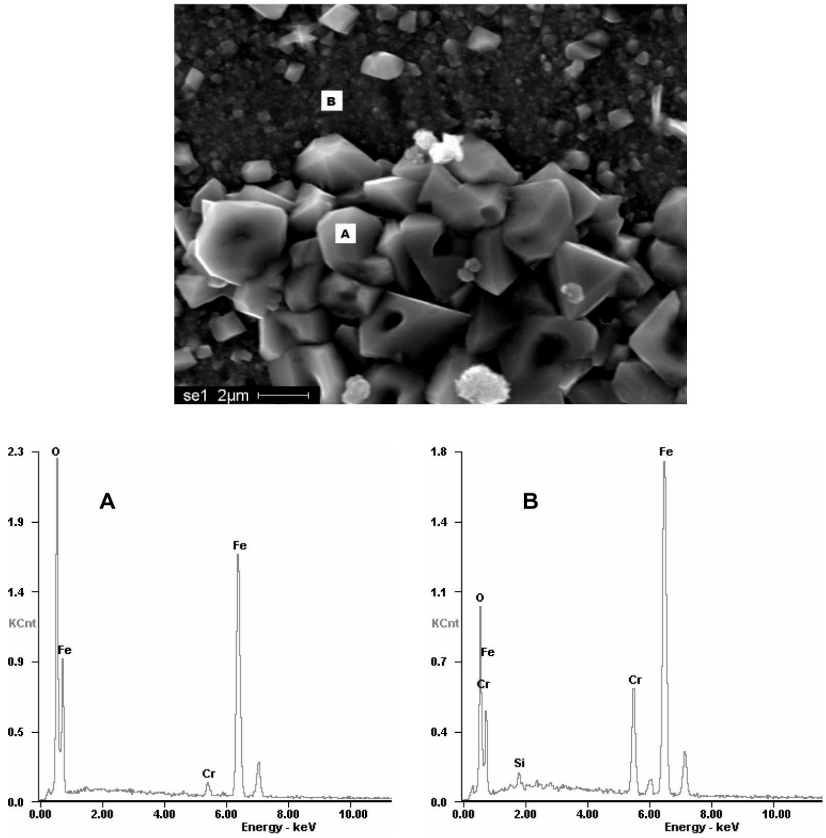

Fig. 7. EDS Analysis of the Oxide Film of the 410 Steel Exposed to SCW at 480 ºC/25 MPa for 500 h

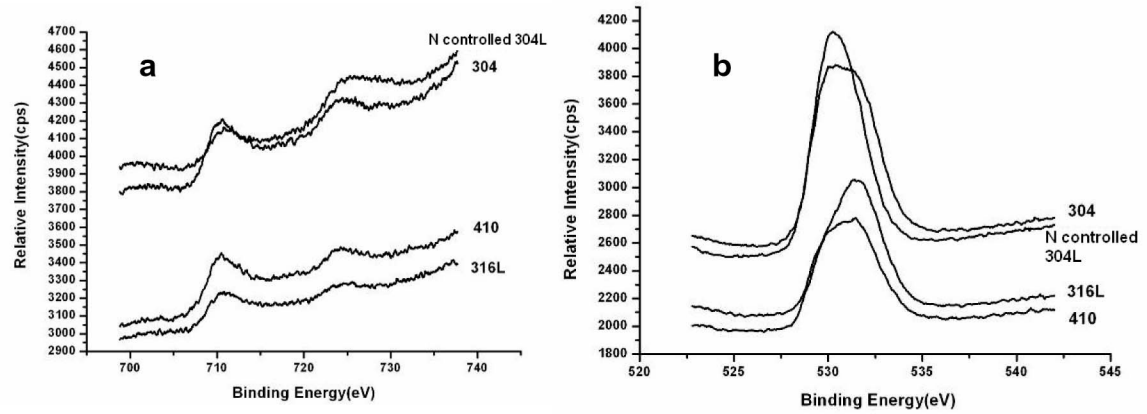

Fig. 8. XPS Spectra of the Stainless Steels Exposed to SCW at 480 ºC/25 MPa for 500 h: (a) Fe and (b) O

Table 2. Binding Energy of XPS Spectra of Stainless Steels Exposed to SCW for 500 h

Element	Fe		O	Cr	
Binding energy	$2p_{3/2}$	$2p_{1/2}$	1s	$2p_{3/2}$	$2p_{1/2}$
316L	710.74	724.18	530.28	576.78	587.21
304	710.66	724.28	530.06	576.59	586.26
N controlled 304L	710.75	724.42	530.04	576.80	586.41
1Cr13	710.69	724.30	530.20	576.74	586.36

the Fe^{3+} and Fe^{2+} states; the binding energy of O 1s was 530.1 eV, corresponding to the form of O^{2-}. The formation of FeO and Fe_2O_3, or an inverse spinel Fe_3O_4 which is structurally similar to a mixture of FeO and Fe_2O_3 [15], can be confirmed. Table 2 shows that the binding energy of the Cr 2p core level corresponds to Cr^{3+} in Cr_2O_3. However, Ni was not found on the surface of the samples.

The results of the XRD analysis for the samples exposed to SCW for 500 h are shown in Fig. 9. According to the EDS results (Fig. 7) and the weak peaks of Fe_3O_4 and $(Fe,Cr)_3O_4$ which overlap, the oxide layers of 316L, 304, and N controlled 304L are identified to be a mixture of Fe_3O_4 and $(Fe,Cr)_3O_4$, and the oxide of 410 may be composed of a Fe_3O_4 outer layer and an inner layer mixed with Fe_3O_4 and $(Fe,Cr)_3O_4$. This result agrees well with the previous XPS analysis on the surface oxide films. However, the oxide films are too thin to measure the Ni oxide structure using XRD. The Ni is likely to be concentrated at the interface between the oxide and the metal.

3.4 Corrosion Mechanisms

According to the present study, the growth of oxide films on steels in SCW may be attributed to the reaction /diffusion controlling mechanism. During the initial stage of the oxidation process, the growth of the oxide film is controlled by the oxidation reaction of metal, which can account for the large increase in weight loss (Fig. 4). Since Fe and Cr can be oxidized readily by reacting with oxygen to form a barrier layer of Fe and Cr oxides mixed on the sample surface [16], this layer can act as a barrier against metal and oxygen ion contact. The oxide growth in this stage is governed by the outward diffusion of metal ions and the inward diffusion of oxygen. It is believed that the oxidation may be controlled by the diffusion of species through the voids, porosities, and so on of the barrier layer; meanwhile, the weight gain will decrease accordingly. The diffusion coefficients of Fe and Cr are much larger than that of oxygen in the barrier layer [17].

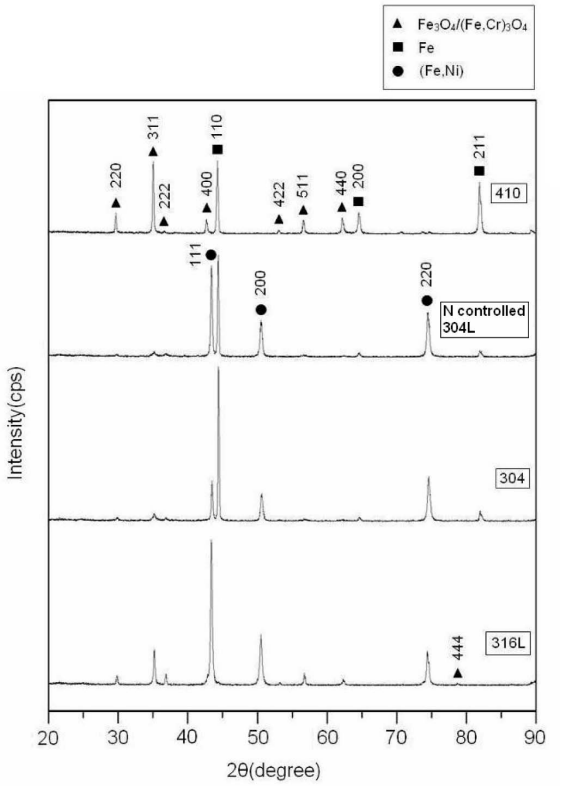

Fig. 9. XRD Results of the Surface of Stainless Steels Tested for 500 h

Therefore, the growth of the barrier layer is due to the outward diffusion of metal ions.

Fe_3O_4 adheres loosely and can be spalled from the substrate easily. As a result of the formation of the $(Fe,Cr)_3O_4$ spinel from the reaction between the Fe_3O_4 and Cr ions, the growth of the oxide layer will become compact. The Cr content of 316L is higher than the ferritic stainless steel, while the Fe content is relatively lower. Therefore, the high corrosion resistance of this steel may be due to the higher content of $(Fe,Cr)_3O_4$ in the oxide layer, which can decrease the outward diffusion rate of the metal ions. However, the lower Cr content of 410 is insufficient to form more spinel. Due to the faster diffusion and higher concentration of Fe [17], the outer porous Fe_3O_4 layer may be formed by the outward diffusion of Fe ions through the inner looser barrier layer. Simultaneously, the formation of this layer will increase the diffusion rate of the metal and oxygen ions. This may be the key reason for the low corrosion resistance of the 410 steel.

The oxide spallation observed in the present study is likely to have resulted from the growth stress during the oxidation process [12]. Loose Fe_3O_4 may be the oxide formed in the initial stage, which spalls easily under stress.

4. CONCLUSION

In deaerated supercritical water at 480 ºC/25 MPa for up to 500 h, 316L steel shows the best corrosion resistance, which may be attributed to its higher Cr and Ni contents. The corrosion resistance of the 410 steel was the worst and may be due to the generation of a loose outer Fe_3O_4 layer, while the other steels have a single layer which are a mixture of Fe_3O_4 and $(Fe,Cr)_3O_4$. The corrosion mechanism of the steels in SCW is likely to be the reaction/diffusion controlling mechanism, while the oxide spallation may be caused by the growth stress.

ACKNOWLEDGEMENTS

This work was supported by the National Basic Research Program of China (2007CB209800). This support is gratefully acknowledged.

REFERENCES

[1] A Technology Roadmap for Generation IV Nuclear Energy Systems, US DOE Nuclear Energy Research Advisory Committee and the Generation IV International Forum, December 2002. Available from http://gif.inel.gov/roadmap.

[2] D. R. Novog, J. Luxat, and L. K. H. Leung. Estimation of conceptual supercritical water reactor response to a small loss of coolant accident. 3rd Int. symposium on SCWR-Design and Technology, 2007: 108-117.

[3] T. C. Totemeier and D. E. Clark. Effect of transient thermal cycles in a supercritical water-cooled reactor on the microstructure and properties of ferritic-martensitic steels, Journal of Nuclear Materials, 2006, 355: 104.

[4] D. Squarer, T. Schulenberg, D. Struwe, et al. High Performance Light Water Reactor. Nuclear Engineering and Design 2003, 221: 167-180.

[5] P. Kritzer. Corrosion in high-temperature and supercritical water and aqueous solutions: a review, Journal of Supercritical Fluids. 2004, 29: 1.

[6] W. Yang, Reactor Material Science, Beijing: Nuclear Energy Press: 195.

[7] Y. Chen, A. Kruizenga, X. Ren, et al. Progress in understanding corrosion in supercritical water systems. 3rd Int. Symposium on SCWR-Design and Technology, 2007: 128.

[8] L. K. Mansur, A. F. Rowcliffe, R. K. Nanstad, et al. Material needs for fusion, Generation IV fission reactors and spallation neutron sources-similarities and differences, Journal of Nuclear Materials, 2004, 329-333: 166-172.

[9] Y. Chen, K. Sridharan, and T. Allen. Corrosion behavior of ferritic-martensitic steel T91 in supercritical water, Corrosion Science, 2006, 48(9): 2843-2854.

[10] X. Ren, K. Sridharan, and T. R. Allen. Corrosion of ferritic -martensitic steel HT9 in supercritical water. Journal of Nuclear Materials, 2006, in press.

[11] L. Tan, Y. Yang, T. R. Allen. Oxidation behavior of iron-based alloy HCM12A exposed in supercritical water. Corrosion Science, 2006, 48(10): 3123-2138.

[12] L. Tan, K. Sridharan, and T. R. Allen. The effect of grain boundary engineering on the oxidation behavior of INCOLOY alloy 800H in supercritical water. Journal of Nuclear Materials, 2006, 348: 263-271.

[13] Assessment and management of ageing of major nuclear power plant components important to safety: PWR vessel internals. IAEA, 1999:14-18.
[14] E. Jiang, W. Yan, R.-C. Liu, et al. Research on general corrosion property of 304NG stainless steel. Nuclear Power Engineering, 2005, 26(4): 390.
[15] C. M. Abreu, M. J. Cristóbal, R. Losada, et al. Comparative study of passive films of different stainless steels developed on alkaline medium. Electrochimica Acta, 2004, 49: 3052.
[16] X. Gao, X. Wu, Z. Zhang, et al. Characterization of oxide films grown on 316L stainless steel exposed to H_2O_2-containing supercritical water. Journal of Supercritical Fluids, 2007, 42: 157-163.
[17] J. Zhang, N. Li, Y. Chen, et al. Corrosion behaviors of US steels in flowing lead-bismuth eutectic (LBE). Journal of Nuclear Materials, 2005, 336: 1-10.